



ELSEVIER

Contents lists available at ScienceDirect

## Materials Science in Semiconductor Processing

journal homepage: [www.elsevier.com/locate/mssp](http://www.elsevier.com/locate/mssp)

# Plasmon spectroscopy of graphene and other two-dimensional materials with transmission electron microscopy

Antonio Politano<sup>a,\*</sup>, Gennaro Chiarello<sup>a</sup>, Corrado Spinella<sup>b</sup>

<sup>a</sup> Università della Calabria, Dipartimento di Fisica, via ponte Bucci, cubo 31/C, 87036 Rende, CS, Italy

<sup>b</sup> CNR-IMM Zona Industriale, Strada VIII 5, 95121 Catania, Italy

## ARTICLE INFO

## Article history:

Received 4 February 2016

Received in revised form

29 April 2016

Accepted 4 May 2016

## Keywords:

Two-dimensional materials

Electron energy loss spectroscopy

Plasmons

## ABSTRACT

Investigations on plasmonic modes of graphene, topological insulators, black phosphorus, boron nitride and two-dimensional carbides by means of transmission electron microscopy are here reviewed. Electron energy loss spectroscopy with atomic resolution allows observing the enhancement of graphene plasmons at substitutional atoms. For topological insulators, the two existing modes in the ultraviolet range have different dispersion relation, thus evidencing band-structure effects on plasmon dispersion. Multiple plasmonic modes in the visible range have been revealed in topological-insulator nanoplatelets. Concerning black phosphorus, the plasmonic spectrum changes with thickness: while the bulk is characterized by a single plasmon mode around 20 eV, other low-energy interband plasmons emerge in few layers. Likewise, an additional mode at 7.5 eV is present in the plasmonic spectrum of few-layer hexagonal boron nitride ((h-BN)). Interband plasmons in graphene, (h-BN), or transition-metal dichalcogenides exhibit frequency dependence on thickness. Such a phenomenon is absent in two-dimensional carbides, for which the bulk plasmon does not change with thickness, while the surface plasmon can be tuned by chemical functionalization and/or thickness.

Published by Elsevier Ltd.

## 1. Introduction

Plasmons represent stand-alone solutions of Maxwell's equations. In a plasmonic excitation, valence electrons are involved in a longitudinal oscillation, where electrons coherently move with the same values of both frequency and wave-vector [1–9]. Research on plasmon modes and their applications has originated the field of plasmonics [10–15].

While electron energy loss spectroscopy (EELS) in reflection is more suitable for investigating surface [4,6] and two-dimensional (2D) [16,17] plasmons, EELS in transmission mode can provide a complete information on plasmon modes at higher energy [18–24].

EELS with transmission electron microscopy (EELS-TEM) can be used to measure electronic properties with atomic resolution [25,26]. After several decades of development [27], EELS-TEM currently is characterized by a spatial resolution down to 0.1 nm with an energy resolution down to 0.1 eV. Therefore, nowadays EELS-TEM is a valuable technique for investigations in nanoplasmonics [28]. As a matter of fact, EELS-TEM has been recently used for studying plasmons in novel 2D materials: free-standing graphene [29–33], black phosphorus [34–36], topological insulators [37,38],

hexagonal boron nitride [39,40], and two-dimensional carbides [41].

In this review, we present the state-of-art of plasmon spectroscopy with EELS-TEM with layered materials, particularly focusing on 2D semiconductors [42]. For the aim of this review, we consider as two dimensional the materials with highly ordered atomic arrangement and with anisotropic surface chemical bonds, i.e. strong bonds in the in-plane direction and weak van der Waals bonds in the out-of-plane direction [43]. The missing dangling bonds at the surfaces of the sheets enable mechanical exfoliation of bulk crystals down to flakes with thickness of single unit cells [44–55]. Layered materials, even for relatively high thickness compared with the single-unit-cell flake ( $\sim 10$  nm), are characterized by a substantially anisotropic behavior of their properties (in-plane vs. out-of-plane) [56–60]. The isolation of few-layer samples also introduces quantum confinement in the vertical direction [61,62], which has a notable influence on the band-gap of the material [63,64].

In all EELS-TEM studies on graphene and 2D semiconductors, plasmon modes are originated by interband transitions in the ultraviolet region of the electromagnetic spectrum [65]. While the study of plasmons in the terahertz range [16,66,67] is inhibited because of the insufficient energy resolution, EELS-TEM investigations on valence-band excitations are crucial for the promising prospect of ultraviolet plasmonics [68–72].

\* Corresponding author.

E-mail address: [antonio.politano@fis.unical.it](mailto:antonio.politano@fis.unical.it) (A. Politano).

## 2. Graphene

Plasmonic excitations in graphitic systems arise from the collective electronic excitations of the  $\pi$  valence electrons ( $\pi$  plasmon at 6–12 eV) and of all valence electrons ( $\sigma+\pi$  plasmon at 27–32 eV).

For the cases of momentum transfers parallel to graphite plane, only interband transitions between states with same parity ( $\pi \rightarrow \pi^*$  and  $\sigma \rightarrow \sigma^*$ ) are permitted [31,73] (Fig. 1). The  $\pi \rightarrow \pi^*$  transition, with maximum joint density of states (JDOS) in the nearness of the M point of the Brillouin zone, originates the  $\pi$  plasmon. Similar excitations are proper also of other carbon nanosystems, i.e. fullerenes [74,75] and carbon nanotubes [76,77].

In Table 1 we report the  $\pi$ -plasmon energy at  $q \approx 0$  for various carbon-based systems, as well as the full-width at half maximum (FWHM) of the plasmonic peak. The energy of the  $\pi$  plasmon ranges between 4.7 eV (free-standing graphene) [78] and 6.5–7.0 eV (graphite) [79]. Between these two extreme values, intermediate values have been reported for the cases of vertically aligned (VA) single-walled carbon nanotubes (SWCNT) [78], single-layer graphene on 6H-SiC(0001) [80] ( $\sim 5$  eV), and magnetically aligned bundles of SWCNT [81] ( $\sim 6$  eV).

The  $\sigma+\pi$  plasmon in monolayer graphene has an energy of 14.6 eV [80].

The energy of both  $\pi$  and  $\sigma+\pi$  plasmons increases in graphene multilayers, showing a linear increase with the number of graphene layers, as shown for both free-standing membranes (Fig. 2(a)) and for epitaxial graphene (Fig. 2(b)). The thickness dependence of  $\pi$ -plasmon energy (at small values of the momentum) is determined by the decreasing effect of the screening and of the interlayer coupling by reducing the number of graphene layers [16]. Such effects also influence the dispersion relation of plasmon modes.

Fig. 3(a) shows an electron diffraction pattern for monolayer graphene. Scattering angles are selected by putting a slit above the EELS spectrometer. This allows obtaining momentum-resolved EELS spectra. Therefore, the area covered by the slit defines an area in the reciprocal space, spanned by the spectrometer to provide a momentum-resolved EELS spectrum [88]. The orientation of the specimen and the scattering geometry of the momentum-resolved EELS experiment on monolayer graphene are shown schematically in Fig. 3(c). In the experimental apparatus, the transmission of fast

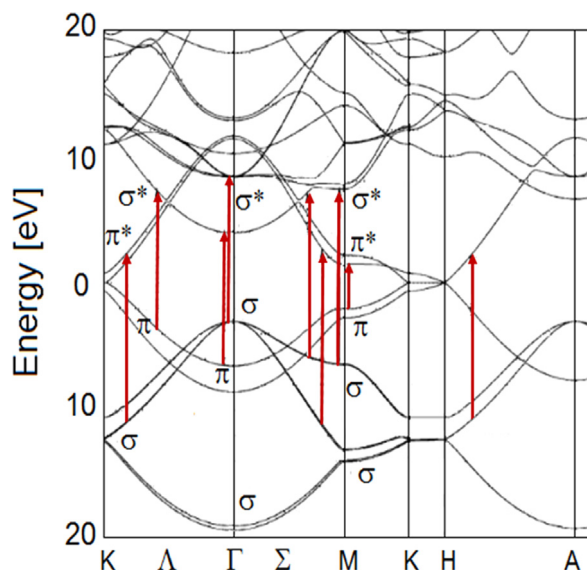


Fig. 1. Electronic band structure of graphite along the Brillouin zone. Interband transitions are indicated with arrows. Adapted from Ref. [65].

Table 1

Energy and line-width of the  $\pi$  plasmon in the long wavelength limit (small momenta) for different systems.

	$E_{\text{loss}}(q=0)$ in eV	FWHM ( $q=0$ ) in eV
Free-standing graphene (theory [78,82] and experiments [31])	4.7 [31] $\sim 6$ [82]	0.45
Monolayer graphene/6 h-SiC(0001) [80]	4.9	0.95
VA-SWCNT [78]	5.1	1.00
Bilayer graphene on SiC(0001) [80]	5.3	1.10
Magnetically aligned bundled SWCNT [81]	6.0	1.25
Graphene/Pt(111) [83]	6.2	1.40
3–4 Layers graphene on SiC(0001) [80]	6.3	1.70
Graphite [79,84–86]	6.5 [79,84] $\sim 7$ [85,86]	2.90
Graphene/Ni(111) [87]	6.7	$\sim 3$

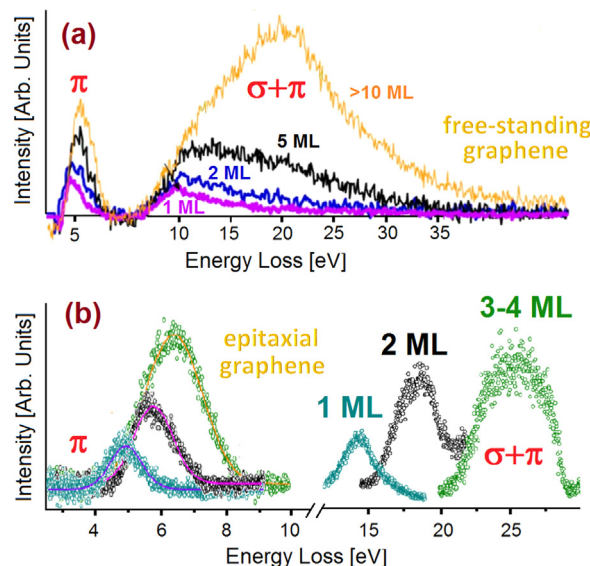


Fig. 2. EELS spectra in the region of  $\pi$  and  $\sigma+\pi$  plasmons for different thickness of graphene sheets for the cases of: (a) free-standing graphene flakes (adapted from Ref. [31]); (b) epitaxial graphene on SiC (adapted from Ref. [80]). ML stands for monolayer.

electrons through a free-standing single layer of graphene occurs. The scattered electrons are analyzed with respect to the energy loss as a function of the scattering angle,  $\theta$ , which is related to the momentum transfer  $q$ , given by:

$$q = k_0 - k'$$

where  $k_0$  and  $k'$  are the wave vectors of incident and inelastically scattered electrons, respectively [89]. The vector  $q$  is decomposed into  $q_{\parallel}$ , the component parallel to the direction of the electron beam (providing momentum transfer perpendicular to the graphene sheet), and  $q_{\perp}$ , the component perpendicular to the electron beam (providing momentum transfer in the plane of the graphene sheet). For  $|q| \ll |k_0|$ ,  $q_{\perp} \approx k_0 \sin\theta$  and  $q_{\parallel} = k_0(\Delta E/2E_0)$ , where  $\Delta E$  is the energy loss and  $E_0$  is the primary electron beam energy. For the energies losses in the range of ultraviolet plasmons,  $\Delta E/2E_0$  is insignificant and, thus, the momentum transfer is contained in the graphene plane ( $q_{\perp}$ ).

Fig. 4 reports the momentum-resolved EELS spectra acquired for monolayer graphene. With increasing momentum transfer, the intensity of the loss features decreases.

The spectra show two dispersing plasmonic features, arising from the  $\pi$  and the  $\sigma+\pi$  plasmons, respectively. The  $\pi$ -plasmon energy linearly increases with increasing values of the momentum  $|q|$ , as

Download English Version:

<https://daneshyari.com/en/article/5006062>

Download Persian Version:

<https://daneshyari.com/article/5006062>

[Daneshyari.com](https://daneshyari.com)